Global Analysis of Dynamic Light Scattering Autocorrelation Functions

Stephen W. Provencher*, Petr Štěpánek**

(Received: 28 June 1995; resubmitted: 12 August 1996)

Abstract

Dynamic light scattering has become a standard technique for investigating colloidal suspensions and polymer solutions. The experimental field autocorrelation function $\hat{g}_1(t)$ can often be well modelled by a Laplace transform relating $\hat{g}_1(t)$ to a distribution of decay times $A(\tau)$. In simple systems $A(\tau)$ can usually be directly related to a distribution of molecular weights, particle sizes, diffusion coefficients or other physically relevant quantities. With constrained regularization methods, the parameter-free estimation of $A(\tau)$ has become straightforward. In complex systems, the resulting $A(\tau)$ may contain several components the identification of which is not always obvious. The problem often originates in a superposition of diffusive and angle-independent components that have different variations of their respective decay times with the scattering vector. A method is presented based on a simultaneous fit of several autocorrelation functions measured at several different scattering angles, which, using simple and reasonable assumptions, yields a robust analysis of the spectra of decay times. The application of the method is illustrated on simulated autocorrelation functions and also on real experimental data obtained on a variety of different polymer systems.

1 Introduction

Dynamic light scattering has become a standard technique for investigating colloidal suspensions and polymer solutions. The experimental field autocorrelation function $\hat{g}_1(t)$ can often be well modelled by a Laplace transform:

$$\hat{g}_1(t) = \int A(\tau)e^{-t/\tau}d\tau. \tag{1}$$

In simple systems, $A(\tau)$ can usually be directly related to a distribution of molecular weights, particle sizes, diffusion coefficients or other physically relevant quantities. With constrained regularization methods, the parameter-free estimation of $A(\tau)$ has become straightforward (for a recent review, see Ref.[1]).

With wide-band correlators, covering many decades in delay time, t, the dynamics of more complex systems are studied. Here, the complexity of $A(\tau)$ and the processes being studied can make the physical interpretation of $A(\tau)$ more difficult. If we use parameter-free methods that do not make a priori assumptions about $A(\tau)$, then important trends in the general structure of $A(\tau)$ can sometimes be discovered in a series of experiments with the systematic variation of an external parameter (e.g. the magnitude of the scattering vector, $q = (4\pi n/\lambda)\sin(\theta/2)$, where n is the refractive index, λ the wavelength and θ the scattering angle). For example, modes in $A(\tau)$ with decay times, τ, independent of q have been observed experimentally [1, 2] and predicted theoretically [3], in contrast to the usual diffusive modes with $\tau \sim q^{-2}$.

If we hypothesize (1) that all modes in $A(\tau)$ are either independent of q or diffusive and (2) that the amplitudes of all modes relative to each other are independent of q, then $A(\tau)$ and $\hat{g}_1(t)$ can be decomposed into two components for all values of q:

$$\beta(q)\hat{g}_1(t;q) = \int_0^\infty A_r(\tau)e^{-t/\tau}d\tau + \int_0^\infty A_d(D)e^{-q^2Dt}dD, \tag{2}$$

$$A(\tau;q) = A_r(\tau) + A_d[1/(q^2\tau)] \tag{3}$$

where $A_r(\tau)$ and $A_d(D)$ are the "relaxational" and "diffusive" components, D is an apparent translational diffusion coefficient and $\beta(q)$ is an unknown scale factor (e.g. due to the scattering geometry). All q dependence is explicitly shown in Eqs. (2) and (3); thus $A_r(\tau)$ and $A_d(D)$ are independent of q but $A(\tau,q)$ is not.

In this paper, we show how global analysis of a series of $\hat{g}_1(t;q)$ measured at different q directly yields estimates of $A_r(\tau)$ and $A_d(D)$. If the hypothesis in Eq. (2) is correct, then this decomposition can greatly improve the physical interpretation and resolution of $A(\tau)$. If the hypothesis is wrong, then this will generally be indicated by a poor fit to the data, because the whole series of $\hat{g}_1(t;q)$ must be simultaneously fitted with only two distributions in the global analysis in Eq. (2), rather than the usual case of only one $\hat{g}_1(t;q)$ being fitted with one $A(\tau)$ in Eq. (1). Thus the global analysis is a stringent test of the hypothesis.

* *S. W. Provencher*, Ph.D., Max-Planck-Institut für Biophysikalische Chemie, Postfach 2841, D-37018 Göttingen (Germany).

** *P. Štěpánek*, Ph. D., Institute of Macromolecular Chemistry, Academy of Sciences of the Czech Republic, Heyrovskeho n.2, 162 06 Praha 6 (Czech Republic).

0934-0866/96/0510-0291 $5.00+.25/0

2 Methods

We discretize Eq. (2) to obtain the following:

$$\hat{g}_1(t;q_i) = \sum_{j=1}^{N_{grid}} \tau_j A_r(t_j) e^{-t/\tau_j} + \sum_{j=1}^{N_{grid}} D_j A_d(D_j) e^{-q_i^2 D_j t} + \\ + C_i + [1 - \beta(q_i)]\hat{g}_1(t;q_i), \quad (4)$$

where $i = 1, \ldots, N_{ACF}$ and N_{ACF} is the number of autocorrelation functions with different q values that are to be simultaneously analysed in the global analysis and C_i is the usual Dust term [4–6] that accounts for modes too slow to be observed in the experimental delay-time range in $\hat{g}_1(t;q_i)$.

The last term on the right-hand side of Eq. (4) was added to both sides of Eq. (2) to eliminate the unknown scaling factor, $\beta(q_i)$, on the left in Eq. (2). The factors $[1-\beta(q_i)]$ are treated as linear parameters to be estimated, just as the usual Dust terms, C_i. However, it is first necessary to replace the model, $\hat{g}_1(t;q_i)$, with the noisy data, $g_1(t,q_i)$, in this last term on the right, so that the parameter $[1-\beta(q_i)]$ occurs only linearly, rather than being multiplied by parameters in $\hat{g}_1(t;q_i)$. This linearizing approximation is not serious with the typical high signal-to-noise ratios in DLS. For one i, say $i = m$, $\beta(q_m)$ is set to 1.0; then the other $\hat{g}_1(t,q_i)$ are automatically scaled with $\beta(q_i)$ in the analysis to match this reference $\hat{g}_1(t;q_m)$. The choice of m is unimportant.

Except for this consistent scaling and weighting of multiple experimental curves, which is implemented in the Splice Package [7] of CONTIN, the modifications for the global analysis are straightforward. There are now two separate grids, one for $\tau A_r(\tau)$ and one for $DA_d(D)$.

Sensitive measures of the consistency of the hypothesis in Eq. (2) with the global analysis are given by the so-called incompatibility ratios:

$$R_i = VAR_i^{global} \quad / \quad VAR_i^{single} \quad (5)$$

where

$$VAR = \sum_{k=1}^{N_{data}} [g_1(t_k) - \hat{g}_1(t_k)]^2/\sigma_k^2, \quad A(\tau_j) \geq 0, \quad (6)$$

and σ_k is proportional to the standard deviation of the noise in the data point $g_1(t_k)$. In the case of the global fit, N_{data} is the total number of data points in all correlation functions. Thus R_i measures the relative deterioration in the fit to ith ACF due to the hypothesis in Eq. (2). If no R_i is significantly greater than 1.0, then the hypothesis is completely consistent with the data. The sensitivity of the R_i increases statistically with N_{ACF}, the range of the q_i and the accuracy of the data. Of course, when the data are very accurate, R_i becomes oversensitive, and better criteria are simply the standard deviations of the global fit to each ACF.

3 Results and Discussion

3.1 Simulated Data

Simulated forms of $A_r(\tau)$ and $A_d(D)$ were specified and Eq. (2) was integrated accurately to obtain a noise-free $g_1(t;q)$, which was substituted in

$$G_2(t;q) = 10^6[1 + [0.7g_1(t;q)]^2]. \quad (7)$$

Poisson noise [5] was then added to $G_2(t;q)$ and the noisy $g_1(t;q)$ was computed. For each ACF, delay times were in 14 groups of eight t values, with the first group in equal intervals from 6.4 to 12 μs and each successive group with 2t of the preceding group. Figure 1 shows the global analysis of simulated data with five scattering angles, θ, equally spaced from 60° to 120°. Both $A_1(\tau)$ and $A_d(D)$ are Gaussians in $\ln(\tau)$ and $\ln(D)$ with equal amplitudes and standard deviations of 0.333 decades.

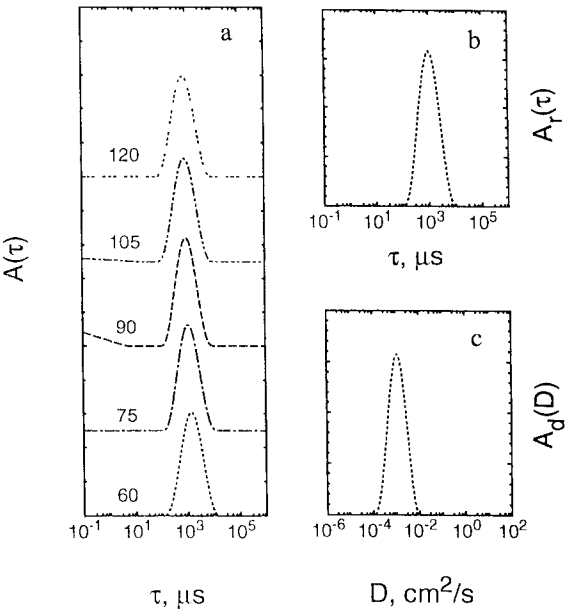

Fig. 1: CONTIN fit to simulated autocorrelation functions for (a) single ACF analysis at each angle indicated, and global analysis as described in the text yielding (b) the relaxational part of the spectrum of decay times and (c) its diffusional part.

The mean of $A_d(D)$ was chosen so that the two distributions exactly overlap at $q = (q_1 q_5)^{0.5}$, or $\theta = 82°$. However, it is clear from Figure 1c that no conventional single-q analysis of one ACF at any of the angles could give an indication of more than one process, since even the exact distributions are unimodal. Only the global analysis can resolve the two processes (peaks). The incompatibility ratios in Eq. (5) were all between 0.99 and 1.02, indicating complete consistence of the hypothesis in Eq. (2) (which of course was used to simulate the data in the first place). In 10 replicate simulations, the root-mean-square deviation from the true values of the amplitude, mean and standard deviation was only 0.7%, 0.2% and 1.7% for $A_r(\tau)$ and 1.2%, 0.4% and 2.1% for $A_d(D)$, respectively. This high accuracy is typical of CONTIN estimates of macroscopic properties [8] of peaks, such as cumulants and moments, despite the large uncertainties in solutions to such ill-posed problems on the microscopic (single-grid-point) scale. Clearly, the accuracy improves with increasing N_{ACF} and range of q. However, the improvement with increasing q range is surprisingly small, although τ of a diffusional mode only varies over a factor of 3.0 when θ varies from 60° to 120°. Hence there is no need to go to extreme values of θ, where there is a danger of systematic experimental errors. A θ range of 30–150° is probably often reasonable. In principle, it is most efficient to space θ so that ln(q) is in equal intervals. N_{ACF} should be at least five, preferably more.

In the following we present a brief illustration of the application of the method to selected cases of dynamic light scattering data on polymer systems. A more extensive and complete discussion will be published elsewhere [9].

3.2 Semidilute Solutions

Semidilute solutions at theta temperature were the first systems where the need for a global analysis became apparent. Figure 2a shows a typical singe-q analysis of an ACF for polystyrene ($M_w = 3.8 \times 10^6$) in cyclohexane (c = 0.064 g/ml) at the theta temperature of 35 °C. It has been shown [1] that the fastest component is diffusive; it represents the gel diffusion coefficient of the semidilute solution. The slowest component was shown to be independent of q [1]; it corresponds to structural relaxation and it was subsequently established that this relaxation time corresponds closely to the slowest relaxation obtained by dynamic mechanical measurements on equivalent solutions [10]. Less clear was the additional intermediate structure in the τ range 10^3–10^4 μs in Figure 2a. It was generally speculated that this was a continuation of the q-independent spectrum due to structural relaxations at distances shorter than the whole chain, and that the extra peaks observed in Figure 2a were artifacts of the regularization method..

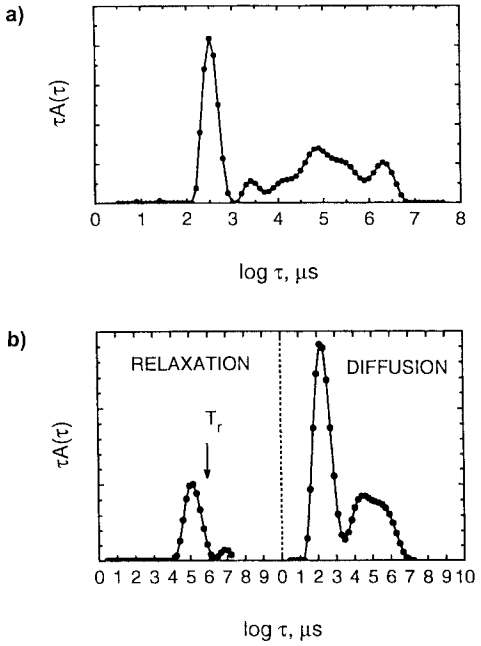

Fig. 2: (a) Spectrum of decay times obtained for the solution of polystyrene ($M_w = 3.8 \times 10^6$) in cyclohexane at 35 °C at a scattering angle of 90°. (b) Global fit to autocorrelation functions obtained on the same solution at several scattering angles as indicated in the text. T_r indicates the longest viscoelastic relaxation time.

Figure 2b shows a similar solution from the global analysis, on a set of correlation functions measured with 12 different scattering vectors. The incompatibility ratios, R_i, range from 1.0 to 2.7, indicating that the model used is acceptable and that the hypothesis seems to agree fairly well with the data. The relaxational component in Figure 2b represents about 30% of the total amplitude and spans about 2.5 decades in τ. The longest viscoelastic relaxation time, T_r, interpolated for this solution from dynamic mechanical measurements [10] (indicated by the arrow) closely corresponds to the longest decay time in $A_r(\tau)$. Figure 2b also indicates that, besides the gel diffusion process, there is a second slow diffusional process with about 20% of the total amplitude. This second slow diffusion is tentatively assigned to structural inhomogeneities, as reported elsewhere [11]. The critical assumption of the independence of the relative amplitudes on q also seems justified. It will be shown in a forthcoming paper that this slower diffusional component consistently appears in semidilute solutions, even in good solvents, and that its amplitude increases beyond that in Figure 2b below the theta temperature.

3.3 Plasticized Polymers

A system with polystyrene plasticized with diethyl malonate (composition 70:30) was prepared by thermal polymerization. The glass transition temperature, T_g, of this system is approximately −50 °C. In a limited range above T_g, fluctuations in density enter into the time window of DLS. On the other hand, since the system still contains a significant portion of solvent, fluctuations in concentrations are expected to be still detectable.

Figure 3 shows the global analysis of ACFs of this system at 5.1 °C with four angles ranging from 30° to 140° in the VV geometry. Two dominant components are resolved, the q-independent relaxation of density fluctuations in $A_r(\tau)$ and the diffusive decay of concentration fluctuations in $A_d(D)$. Here the global analysis is particularly useful, since the two components have similar τ values and, at several scattering angles, the conventional analysis of the ACF at a single angle yields just a broad mixed mode.

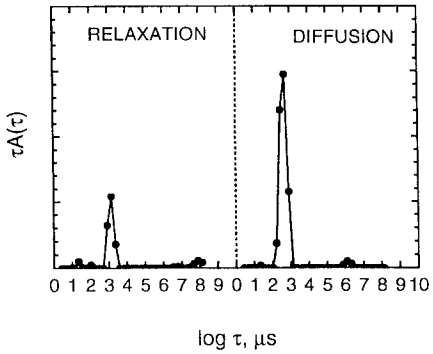

Fig. 3: Distribution of relaxation times obtained from the global fit on a concentrated solution of polystyrene in diethyl malonate (composition 30:70) at a scattering angle of 90°.

3.4 Microemulsion Networks

In contrast to the above two examples, this third example illustrates the rigour of the global analysis in rejecting the hypothesis in Eq. (2) when it is inconsistent with the data. A microemulsion network was formed [12] with a triblock copolymer, poly(oxyethylene)-*block*-poly(isoprene)-*block*-poly(oxyethylene), dissolved in a water-in-oil microemulsion stabilized with AOT (sodium 1,2-bis(2-ethylhexylcarbonyl)-1-ethanesulfonate). The hydrophilic outer blocks dissolve in water droplets; the hydrophobic inner block remain in the oil phase and link the structure in a loose network. ACFs were measured at 10 scattering angles and treated by the global analysis technique. Figure 4 shows large deviations between the fit from the global analysis and the data at large delay times, indicating that the angular variation of at least one slow component cannot be accommodated by Eq. (2). The incompatibility ratios in Eq. (5) range from 2 to 18, clearly rejecting the hypothesis. The corresponding solution in Figure 5 shows two components in the relaxational spectrum and a complex structure in the diffusional part. Since the fit to the data in Figure 4 is fairly good for $\tau < 10^5$ μs, one might speculate that the

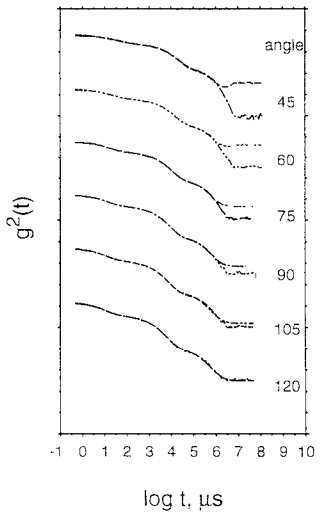

Fig. 4: Autocorrelation functions and fitted curves obtained on a microemulsion network, as in Figure 5. At each angle, the measured data are the lower curve at long delay times.

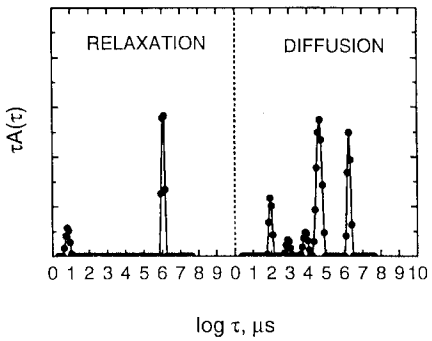

Fig. 5: Distribution of relaxation times obtained on a microemulsion network of a block copolymer, as defined in the text, at a scattering angle of 90°.

corresponding part of the solution with decay times shorter than about 10^5 μs might be real. Work is in progress to elucidate this question.

4 Concluding Remarks

We have shown that by fitting simultaneously correlation functions obtained at various scattering angles, more detailed and precise information can be obtained on the number and character of dynamic processes present in the particular polymer system. We have shown that the hypothesis of the same angular variation of the amplitudes of various dynamic modes is not a very limiting factor and that cases where the hypothesis fails can be clearly detected.

5 Acknowledgements

Cooperation with Dr. *Hofmeier* in providing experimental data from Ref. [12] used here in Section 3.4 is gratefully acknowledged. We also gratefully acknowledge the support of this work by the Grant Agency of the Academy of Sciences of the Czech Republic under Grant No. 450416 (1994) and by the Grant Agency of the Czech Republic under Grant No. 203/94/0817 (1994).

6 Symbols and Abbreviations

$A(\tau)$	distribution of relaxation times
c	concentration
D	diffusion coefficient
DLS	dynamic light scattering
$g_1(t)$	field autocorrelation function
$G_2(t;q)$	intensity autocorrelation function
M_w	weight average molecular weight
n	refractive index
q	scattering vector
R	incompatibility ratio
t	delay time
T_g	glass transition temperature
T_r	longest viscoelastic relaxation time
θ	scattering angle
λ	wavelength of light
σ	standard deviation
τ	relaxation time
ACF	autocorrelation function
AOT	[sodium 1,2-bis(2-ethylhexyl-carbonyl)-1-ethanesulfonate]
VV	vertical-vertical

7 References

[1] *P. Stepanek:* Data Analysis in Dynamic Light Scattering, in *W. Brown* (ed.): Dynamic Light Scattering. The Method and Some Applications. Oxford University Press, Oxford 1993, pp. 177–241.

[2] *T. Nicolai, W. Brown, R. Johnsen, P. Stepanek:* Dynamic Behaviour of Theta Solutions of Polystyrene Investigated by Dynamic Light Scattering. Macromolecules *23* (1993) 1165–1174.

[3] *F. Brochard, P. G. de Gennes:* Dynamical Scaling for Polymers in Theta Solvents. Macromolecules *10* (1977) 1157–1161.

[4] *S. W. Provencher, J. Hendrix, L. De Maeyer, N. Paulessen:* Direct Determinations of Molecular Weight Distribution of Polystyrene in Cyclohexane with Photon Correlation Spectroscopy. J. Chem. Phys. *69* (1978) 4273–4276.

[5] *S. W. Provencher:* Inverse Problems in Polymer Characterization: Direct Analysis of Polydispersity with Photon Correlation Spectroscopy. Macromol. Chem. *180* (1979) 201–209.

[6] *S. W. Provencher:* CONTIN – A General Program for the Regularized Solution of Linear Integral Equations. Comput. Phys. Comm. *27* (1982) 213–229.

[7] *S. W. Provencher:* CONTIN Update 2; MPI für Biophysikalische Chemie, Göttingen, 1991.

[8] *S. W. Provencher:* Low-bias Macroscopic Analysis of Polydispersity, in *S. E. Harding, D. B. Satelle, V. A. Bloomfield* (eds.): Laser Light Scattering in Biochemistry. Royal Society of Chemistry, Cambridge 1992, pp. 92–111.

[9] *S. W. Provencher, P. Stepanek:* Macromolecules, in preparation.

[10] *T. Nicolai, W. Brown, S. Hvidt, K. Heller:* A Comparison of Relaxation Time Distributions Obtained from Dynamic Light Scattering and Dynamic Mechanical Measurements for High Molecular Weight Polystyrene in Cyclohexane. Macromolecules *23* (1990) 5088–5096.

[11] *J. T. Koberstein, C. Picot, H. Benoit:* Light and Neutron Scattering Studies of Excess Low-angle Scattering in Moderately Concentrated Polystyrene Solutions. Polymer *26* (1985) 673–681.

[12] *F. Stieber, U. Hofmeier, H. F. Eicke, G. Fleischer:* Diffusion Processes of Interacting Brownian Particles in Block Copolymer-Microemulsion Transient Network. Ber. Bunsenges. Phys. Chem. *97* (1993) 812–818.